



Supplement of

Injection near the stratopause mitigates the stratospheric side effects of sulfur-based climate intervention

Pengfei Yu et al.

Correspondence to: Pengfei Yu (pengfei.yu@colorado.edu)

The copyright of individual parts of the supplement might differ from the article licence.

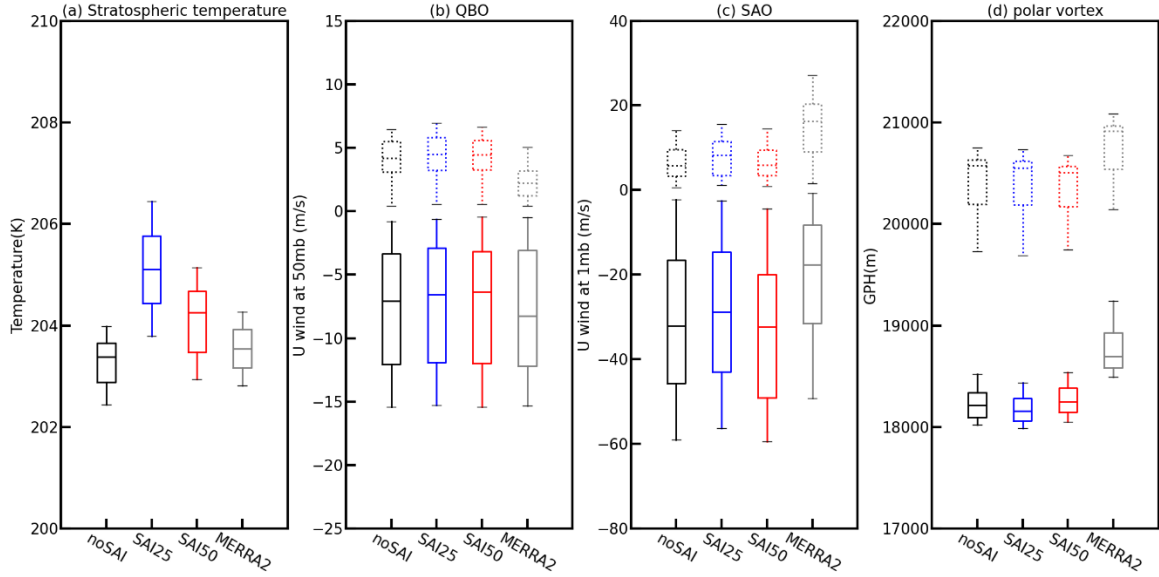


Figure S1: Box plots comparing stratospheric variability between model simulations and MERRA2 reanalysis (2000-2020). (a) near-global (60°S - 60°N) temperatures at 100 mb; (b) Quasi-biennial Oscillation (QBO) strength (tropical zonal mean zonal wind at 50 mb) with east phase (dashed) and west phase (solid); (c) Semiannual Oscillation (SAO) strength (tropical zonal mean zonal wind at 1 mb) with east phase (dashed) and west phase (solid); (d) Antarctic (solid) and Arctic (dashed) polar vortex strength (denoted by the geopotential height averaged over 65°S - 90°S at 50 mb) in the model and MERRA2 reanalysis dataset between year 2000 and 2020. Box plots show the median (horizontal line), 25th-75th percentiles (box), and 5th-95th percentiles (whiskers).

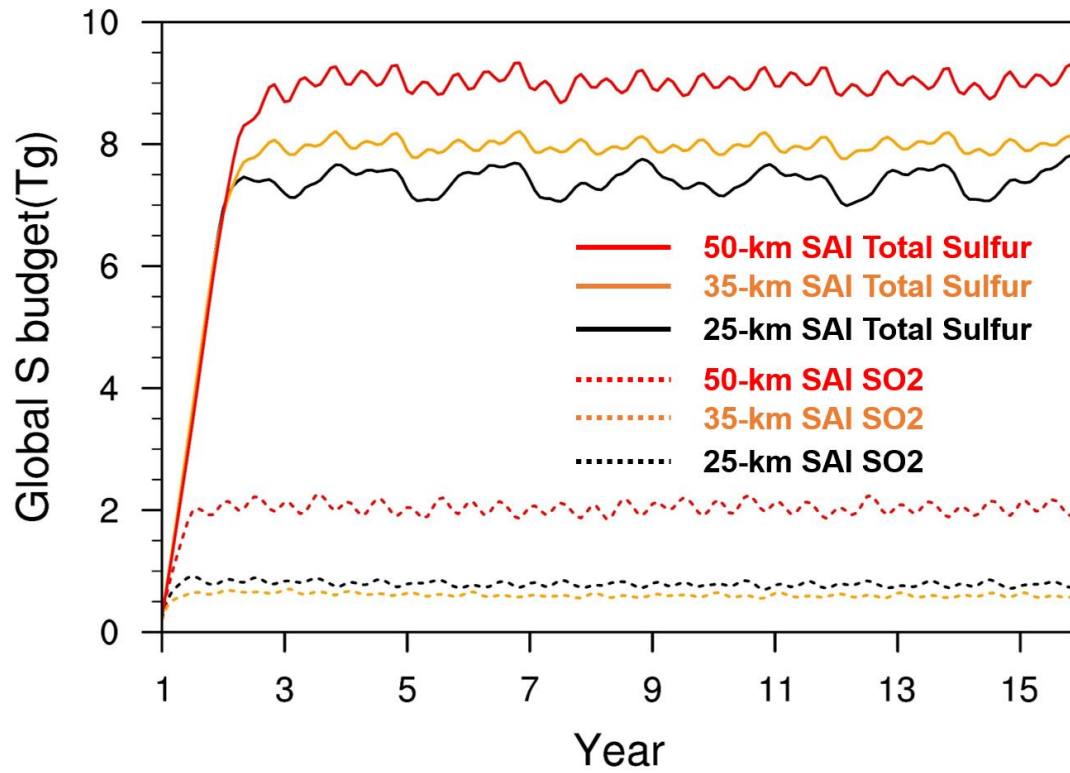


Figure S2: Simulated global stratospheric budget of sulfur (Tg) in SAI experiments with injection heights of 25, 35 and 50 km at 15°N and 15°S. The budget of total sulfur (both in gas and condensed phases) is denoted by solid lines, and the budget of SO₂ gas is denoted by the dashed lines.

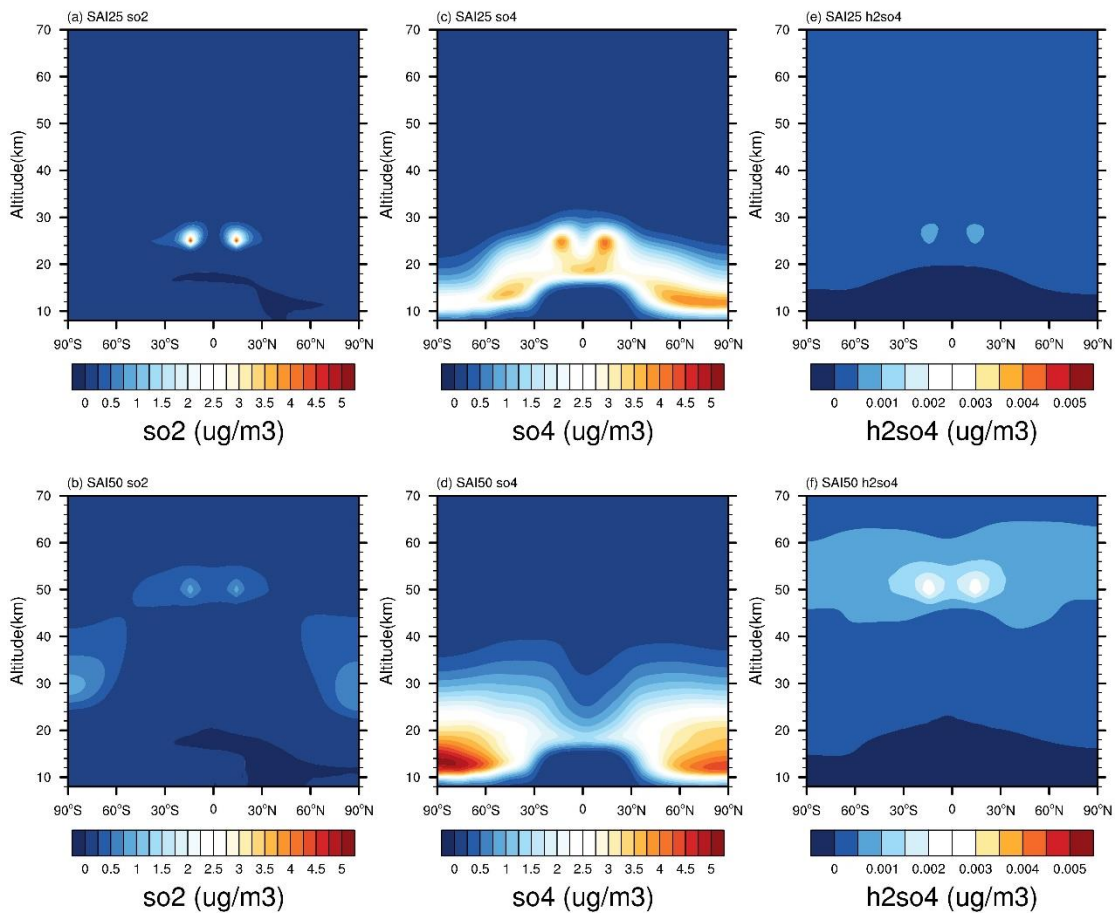


Figure S3: (a) The vertical distribution of the zonal and annual mean SO_2 anomalies in SAI_{25} . (b) same as (a) but for SAI_{50} ; (c-d) same as (a-b) but for sulfate aerosol. (e-f) same as (a-b) but for H_2SO_4 . Note that the contour range in panel (e-f) H_2SO_4 is 3 magnitudes smaller than sulfate and SO_2 .

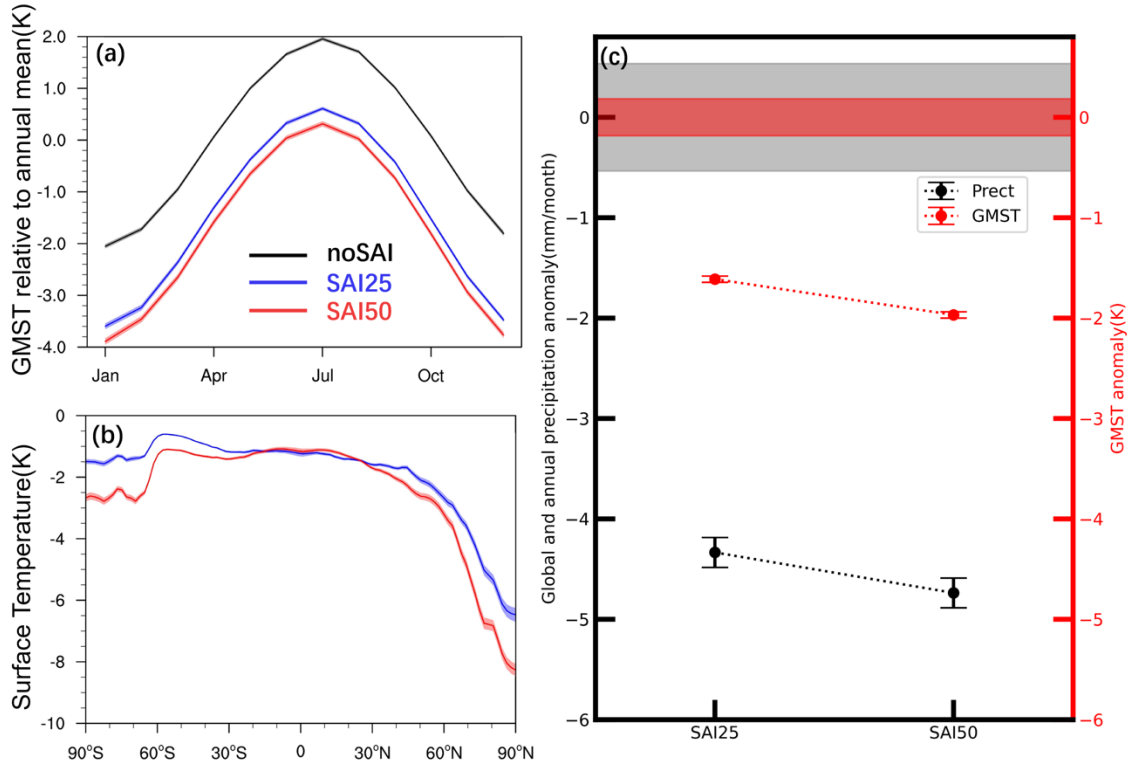


Figure S4: Global surface temperature responses to SAI scenarios. (a) Seasonal cycle of global mean surface temperature (GMST) relative to the annual mean among control (in black), SAI₂₅ (in blue) and SAI₅₀ (in red) simulations. The shadings of each line represent the ensemble standard deviation of the mean; (b) zonal mean surface temperature anomalies relative to the control simulations for SAI₅₀ (red) and SAI₂₅ (blue) scenarios. The shadings of each line represent the ensemble standard deviation of the mean; (c) GMST anomalies for SAI₂₅ and SAI₅₀ scenarios (red dots, right axis) with error bars showing ensemble standard deviation of the mean from 45-member simulations. Global mean precipitation anomaly for SAI₂₅ and SAI₅₀ scenario (black dots, left axis) with error bars showing ensemble standard deviation of the mean. The magnitude of natural variabilities (one standard deviation) of GMST and precipitation rate from the control simulations are shown in red and black shadings, respectively.

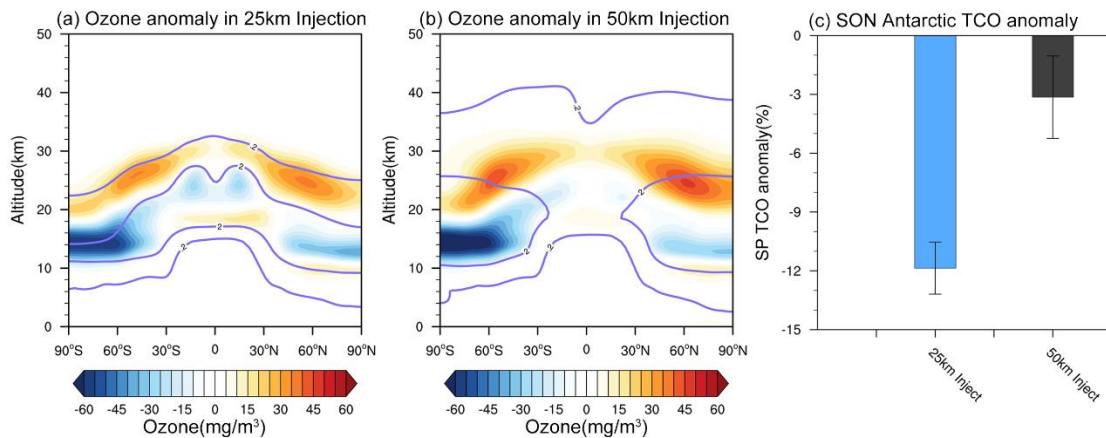


Figure S5: (a) Simulated annual mean ozone anomalies due to 25-km injection SAI under the ozone depleting substance (ODS) conditions of year 2040 relative to the simulations without SAI. The simulated annual mean aerosol concentrations of 12 and 2 $\mu\text{g m}^{-3}$ are denoted by the contour lines; (b) same as (a) but for the simulated ozone anomalies due to 50-km injection SAI (SAI₅₀); (c) Simulated Antarctic (60°S-90°S) column ozone anomaly averaged from September-October-November (SON) from SAI scenarios with different injection altitudes (at 25 km and 50 km) under the ODS conditions of year 2040. The error bars denote the standard deviation of the mean from the ensemble simulations with details in Materials and Methods.